

# Dynamic modeling of the microbial community prior to and during uranium-bioremediation

Kai Zhuang<sup>1\*</sup>, Mounir Izallalen<sup>2</sup>, Paula Mouser<sup>2</sup>, Hanno Richter<sup>2</sup>, Carla Risso<sup>2</sup>, Derek R. Lovley<sup>2</sup>, Radhakrishnan Mahadevan<sup>1</sup>

<sup>1</sup>Department of Chemical Engineering, University of Toronto, Canada

<sup>2</sup>Department of Microbiology, University of Massachusetts, USA

1: University of Toronto  
Department of Chemical Engineering and Applied Chemistry,  
Institute of Biomaterials and Biomedical Engineering,  
Toronto, ON, Canada M5S3E5

2: University of Massachusetts  
Department of Microbiology,  
Amherst, MA, USA 01003

\*Corresponding author

Email: [k.zhuang@utoronto.ca](mailto:k.zhuang@utoronto.ca)

Additional Contacts

Email: [krishna.mahadevan@utoronto.ca](mailto:krishna.mahadevan@utoronto.ca)

Running title: Community modeling of uranium-bioremediation  
Submission to: ISMEJ

## ABSTRACT

We have created a dynamic genome-scale metabolic model of *Geobacter sulfurreducens* and *Rhodospirillum rubrum*, the two primary iron-reducers in uranium-contaminated grounds, in order to understand the community competition prior to and during uranium-bioremediation.

The simulation results agree with experimental measurements, and suggest that the community competition is modulated by two factors: the ability of *G. sulfurreducens* to fix nitrogen under ammonium limitation, and a rate vs. yield trade-off between these two organisms. Prior to acetate amendment, if ammonium is limited, *G. sulfurreducens* dominates due to its ability to fix nitrogen. However, if the system contains abundant ammonium, *R. rubrum*, a yield-strategist, is favoured because the acetate flux is very low. During acetate amendment, the high acetate flux strongly favours *G. sulfurreducens*, a rate-strategist. The model also predicts the up-regulation of respiration in *G. sulfurreducens* during nitrogen fixation by sacrificing its biomass yield, leading to an increase in uranium reduction under low ammonium conditions. This model will be an important tool for the designing of effective uranium-bioremediation strategies.

## INTRODUCTION

The anoxic ferric microbial community contains abundant numbers of *Geobacteraceae* and *Rhodoferrix* species, dissimilatory iron-reducing bacteria capable of extra-cellular electron transfers (Chaudhuri & Derek R Lovley, 2003; Cummings et al., 2003; Methé et al., 2003; Derek R Lovley et al., 2004; Esteve-Núñez et al., 2005; Finneran et al., 2003). These organisms are capable of using uranium(VI) as a terminal electron acceptor; the process converts soluble uranium(VI) to its precipitate form, uranium(IV), thus prevents uranium from entering the ground water stream. There are significant physiological differences between *Geobacter sulfurreducens* and *Rhodoferrax ferrireducens*, the model species of these two genera of iron reducers. Compared to *G. sulfurreducens*, *R. ferrireducens* can oxidize a wider range of substrates, including glucose, using iron(III) as a terminal electron acceptor (Finneran et al., 2003; Chaudhuri & Derek R Lovley, 2003). On the other hand, while *G. sulfurreducens* is dependent on fermenters that supply the typical electron donor for this microorganism, such as acetate and H<sub>2</sub> (Derek R Lovley & Phillips, 1989), it is capable of fixing nitrogen under ammonium deprivation. Furthermore, *G. sulfurreducens* grows faster than *R. ferrireducens* at the cost of energetic efficiency (Chaudhuri & Derek R Lovley, 2003; Finneran et al., 2003; Esteve-Núñez et al., 2005). Acetate amendment has been shown to be an effective bioremediation strategy by stimulate the growth of these iron-reducers; however, after the initial dominance of *Geobacter*, continued acetate injection stimulates the growth of sulfate reducers, causing the reduction of uranium(VI) to stop (Chang et al., 2005; Vrionis et al., 2005; Anderson et al., 2003). In order to devise environmental biotechnology strategies for bioremediation of uranium-contaminated sites (N'Guessan et al., 2008; D R Lovley, 2003), we need a more in-depth understanding of the ecology of this metal reducing community (Figure 1).

Microorganisms in nature exist in complex communities, either in cooperation or in competition. The composition of the community and the metabolic states of its members are highly sensitive to the ever-changing environment. The activities of the community members can modify the environment, which further modifies community composition and behavior. For example, the rumen microbial community composition varies significantly based on the host's dietary input (Tajima et al., 2000), and the community's digestive performance is decided by the community's composition. In addition, given the microbial diversity and abundance (Konopka, 2006), one cannot truly understand nature without understanding microbial communities. However, modeling and physiology studies have mainly focused on pure cultures in the past (McMahon et al., 2007; D R Lovley, 2003).

The advent of systems biology has greatly increased our understanding of the complex processes present at the organism level. Applying a similar systems approach to the study of microbial communities would reveal some insights into the intricate interactions and emergent properties among these communities. (Konopka, 2006) Flux balance analysis is a systems biology modeling methodology that does not require a complete kinetic description, yet is able to incorporate as much genomic and physiological information as possible (Lee et al., 2006). In FBA models, the metabolic pathways are mathematically represented as a stoichiometric matrix. After the applications of thermodynamic and physiologic constraints, linear programming is used to calculate the metabolic fluxes through each of the pathways by assuming a cellular objective function such as the maximization of biomass yield (Jeremy S Edwards et al., 2002; Price et al., 2004; Warren & Jones, 2007). FBA models of pure cultures, such as *Escherichia coli* (Rafael U Ibarra et al., 2002; J S Edwards et al., 2001; Feist & Bernhard Ø Palsson, 2008; Reed & Bernhard Ø Palsson, 2003; Reed et al., 2003; Feist et al., 2007) and *G. sulfurreducens* (R

Mahadevan et al., 2006; Segura et al., 2008), are capable of accurate growth predictions. This modeling approach has been useful for both understanding the behavior of biological systems in complex environment and for engineering purposes (Burgard et al., 2003; Hjersted et al., 2007; Pharkya et al., 2003; Anesiadis et al., 2008; Pharkya & Maranas, 2006; Izallalen et al., 2008).

Previously, Stolyar *et al.* (2007) created the first FBA-based metabolic model of a mutualistic microbial community. In this model, the stoichiometric matrices of *Desulfovibrio vulgaris* and *Methanococcus maripaludis* are connected together directly (Stolyar et al., 2007). The authors assumed that since the two species grew at the same rate, did not explicitly consider the dynamic changes in the biomass concentrations of the individual species. While this approach may be appropriate when the microorganisms are inter-dependent, it is inappropriate in complex ecological settings where the community composition is dynamic.

In this paper, we present a dynamic metabolic model of *G. sulfurreducens* and *R. ferrireducens*, utilizing a dynamic multi-species metabolic modeling framework (DMMM). It is the first model to dynamically integrate multiple genome-scale metabolic models. By modeling the coculture of these two organisms, along with recent physiological and genetic insights, we were able to explain the composition and the dynamic changes in the microbial community prior to and during uranium bioremediation.

## **METHOD**

### **1. The Dynamic Multi-species Metabolic Modeling framework**

A community metabolic model must account for the metabolic exchanges between species and with the environment, as well as the changes in biomass of the relevant species. The

DMMM framework is based on the dynamic flux balance analysis developed by Mahadevan *et al.* (Radhakrishnan Mahadevan et al., 2002; R. Luo et al., 2006). In the DMMM framework, each species is treated as an object containing a metabolic model and a set of operations. The metabolic model can be described either by Monod-kinetic equations or by FBA, so long as the model can predict a set of metabolic exchange fluxes and a biomass flux, given a set of input parameters. The species are embedded inside an environment object. The environment object also contains the metabolite and biomass concentrations inside the environment. The simulation procedure is summarized as the following: [1] the metabolite production/consumption rate is calculated by multiplying the flux with the respective biomass. [2] The sum of production/consumption rates for each metabolite is integrated over the simulation time.

## **2. Modeling the anoxic ferric iron-reducing community**

The well-studied *G. sulfurreducens* and *R. ferrireducens* are used to represent the *Geobacteraceae* and *Rhodoferrax* genera in our study of the anoxic ferric iron-reducing community. The previously published *G. sulfurreducens* genome-scale FBA model (R Mahadevan et al., 2006) was used to represent the *Geobacteraceae* species, and a newly developed *R. ferrireducens* genome-scale FBA model was used to represent the *Rhodoferrax* species. The *Geobacter* model is expanded and updated with the current physiological data - specifically, the cost of nitrogen fixation is increased to 16ATP from 8ATP, based on experimental observations. Maximization of biomass yield is assumed to be the cellular objective for both organisms. The acetate, glucose, Fe(III), Fe(II), CO<sub>2</sub>, NH<sub>4</sub> exchange fluxes of both organisms represent the sources and sinks of metabolites from and into environment for each species.

The DMMM framework is applied to the modeling of this iron-reducing community (Figure 2). As in the dFBA formulation (Radhakrishnan Mahadevan et al., 2002), the flux of primary carbon and the energy source are restricted by their concentrations in the environment using a Michaelis-Menten equation. The acetate transport kinetics of *G. sulfurreducens* has been determined by measuring the C-14 labeled acetate uptake (Richter et al., Personal Communication). Three different acetate uptake mechanisms, each with different  $K_s$  and  $V_{max}$ , were observed in that study. The *G. sulfurreducens* acetate uptake flux in the DMMM framework is constrained by the summation of three experimentally identified Michaelis-Menten expressions. The acetate uptake rate of *R. ferrireducens* is calculated from previously published batch growth data (Finneran et al., 2003), and its  $K_s$  is assumed to be the same as the lowest of the *G. sulfurreducens*  $K_s$ . The ATP maintenance requirement for *G. sulfurreducens* is 0.45 mol ATP/gDw, and the ATP maintenance requirement for *R. ferrireducens* is calculated to 0.7 mol ATP/gDw (Risso et al., Personal Communication).

$$v_{ac}^{Gs} = \frac{14.3S}{S + 0.405} + \frac{2.37S}{S + 0.023} + \frac{1.60S}{S + 0.008}$$

$$v_{ac}^{Rf} = \frac{1.85S}{S + 0.008}$$

### 3. Death phase modeling

Microorganisms enter death phase due to a failure to meet the maintenance energy requirements — neither *G. sulfurreducens* nor *R. ferrireducens* can grow once Fe(III) is depleted. The death rate of an organism has been calculated by multiply the yield (gDw/mol substrate) with the substrate maintenance flux (mol substrate/gDw)(Rittmann & McCarty, 2001; VanBriesen, 2002). We can find the death rate of the organism using the constraint-based metabolic model in a similar fashion. The substrate maintenance flux is the acetate flux needed

to meet the ATP maintenance energy requirements, and can be found by minimizing for acetate while fixing the growth flux to zero. The death rate is calculated as the negative of the growth flux when the acetate uptake flux is set to the maintenance flux and the ATP maintenance requirement is set to zero.

#### **4. Pre-injection simulations**

Prior to acetate injection, acetate is generated in the anoxic sediments as a fermentation product. The uptake rates and concentration of organic chemicals, including acetate, has been determined experimentally in various sediment environments. Although no such experiment was done specifically for the anoxic ferric environment of interest, we can assume the rates and concentration to be very low (King & Klug, 1982; de Graaf et al., 1996). Acetate fluxes of 3  $\mu\text{M}/\text{day}$ , 5  $\mu\text{M}/\text{day}$ , 10  $\mu\text{M}/\text{day}$ , 50  $\mu\text{M}/\text{day}$  are used in the simulations, which is comparable to the acetate that would be generated from the environmental glucose turnover rate. From field experiments (Mousser *et al.*, Personal Communication), we know that the ammonium concentration are typically low, although high ammonium locations do exist occasionally. The steady state ammonium concentration is assumed to be either 0.4 mM or 0.005 mM in order to simulate either ammonium limitation or excess conditions. Fe(III) is assumed to be not limiting prior to injection, and is set to 30 mM. The initial biomass concentration for both *G. sulfurreducens* and *R. ferrireducens* are assumed to be 0.00001g/L, which corresponds to  $10^7$  cells/L. This is a reasonable value for an unamended aquifer with low organic carbon. (cite JCH) Environmental dilution rate is assumed to be 0.01 hr<sup>-1</sup> (Yabusaki et al., 2007).

#### **5. Post-injection simulations**

During the acetate injection field experiment, a high acetate flux is artificially created in order to induce a non-substrate-limiting condition. In our simulation, a very high acetate flux of



1mM/day is used. The ammonium concentration is assumed to be similar to that of the pre-injection situation. While ammonium concentration is mostly very low, there is one significant outlier, well D08, with a maximum concentration of 0.4 mM and an average concentration of 0.3 mM. As with the pre-injection simulations, both ammonium excess and ammonium limiting conditions are simulated. Fe(III) limitation is hypothesized to occur after a prolonged period of acetate injection. Previous sediment sampling at bioremediation sites reports Fe(III) concentration to be in the range of 5 - 40  $\mu\text{mol/g}$  (Anderson et al., 2003; Vrionis et al., 2005; Yabusaki et al., 2007), which includes both bioavailable and non-bioavailable Fe(III). If we assume sediment density to be 2 g/ml and 50% of Fe(III) are bioavailable, 2.5 - 20 mM of Fe(III) is bioavailable. For the post-injection simulations, the initial Fe(III) concentration is assumed to be 10mM (why not use 15 for both post and preinjection simulations rather than 30 there and 10 here...). As with the pre-injection simulations, initial biomass for both organisms are set to 0.00001g/L.

## **6. Validation and sensitivity analysis**

Conditions of test-wells D08 and D05 during 2007 field experiment are simulated. The initial acetate concentration is set to zero, and the initial ammonium concentration is set to the *in situ* measurement values at time zero. The fluxes of ammonium and acetate is determined the solution of the constraint-based metabolic model. The *in silico* acetate injection is stopped at day 10, in accordance with the field-scale experiment. The *in situ* 16S rRNA measurement of *G. sulfurreducens* and *R. ferrireducens* abundance is used to calculate the *G. sulfurreducens* and *R. ferrireducens* fractions at day 0, 9, 18. Simulations are initialized with the *in situ* *G. sulfurreducens* to *R. ferrireducens* ratios (1:4 for D08 and 7:4 for D05). Since we do not know the organisms' biomass without acetate amendment and the bioavailable ferric iron

concentration, we assume that the total biomass prior to injection is in the range of 0.000001 g/L to 0.0001 g/L, and the bioavailable Fe(III) is in the range of 2.5 - 20 mM. Nine simulations are performed at different initial biomass concentrations and Fe(III) concentrations for each well. *Geobacter* fraction, defined as  $[Gs]/([Gs]+[Rf])$ , is used as the metric to compare *in situ* and *in silico* organism abundance.

## RESULTS

### 1. Pre-injection

The microbial competition prior to acetate injection was simulated for 800 hours in eight simulations. The simulations were differentiated by different acetate fluxes and whether ammonium is limiting. The acetate concentration in all eight simulations reached a steady state below 10 nM (Figure3), which is comparable in order of magnitude to previously reported acetate concentrations in relevant environment (de Graaf et al., 1996). In the ammonium excess simulations, ammonium is never exhausted; in the ammonium limiting simulations, ammonium is rapidly exhausted (not shown).

The fraction of *G. sulfurreducens* in the community is a measure of the relative success of the two organisms. A fraction value above 0.5 indicates *Geobacter* success, and a value below 0.5 indicates *Rhodoferrax* success. Since the acetate concentrations reach a steady state by the 800th hour in all simulations, we can assume that the *Geobacter* fraction at this time is indicative of the overall success of the two organisms. This value is dependent on both acetate flux and whether ammonium limitation exists.

In the ammonium excess cases, the *Geobacter* fraction increases as the acetate flux increase, indicating that *G. sulfurreducens* is more successful in environments of higher acetate fluxes. In the ammonium limiting cases, the initial trend is similar until the point at which ammonium is exhausted. After that point, the *Geobacter* fraction increases at a rapid rate (Figure 3). These simulations suggest that *R. ferrireducens* has an advantage over *G. sulfurreducens* in a low substrate flux environment, however, due to its inability to fix atmospheric nitrogen, it cannot compete against *G. sulfurreducens* when ammonium is limited. A similar trend is observed in the *in situ* rRNA samples of *Geobacteraceae* and *Rhodoferrix* species. In well D08, which has a high ammonium concentration, the fraction of *Geobacteraceae* measured prior to acetate injection is 20%. In wells of low ammonium concentrations, including D05 and D02, the measured fractions are 63% and 58% respectively.

## **2. Post-injection**

Microbial competition during acetate-injection bioremediation is simulated for 400 hours in two simulations, differentiated by whether ammonium is in excess or limiting. Both *G. sulfurreducens* and *R. ferrireducens* biomass increase initially; however, *G. sulfurreducens* outcompetes *R. ferrireducens* rapidly after the initiation of acetate injection, indicated by the rapid increase in *Geobacter* fraction value (Figure 4 f). In the simulation with high ammonium concentration and flux, ammonium is never exhausted. In the low ammonium simulation, ammonium is exhausted at around 50 hours. *G. sulfurreducens* enters the nitrogen fixation metabolic state - additional energy is spent on fixing nitrogen, leading to a decrease in biomass production. While *R. ferrireducens* cannot fix nitrogen, it is capable of maintaining its cell mass as maintenance does not require a nitrogen source (Figure 4 b). In both cases, once Fe(III) is exhausted, both organisms enter decay phase. Fe(III) is exhausted slightly later in the nitrogen

limiting case (Figure 4 c). Acetate is never exhausted during the simulation; however, if more Fe(III) is available, acetate can reach exhaustion temporarily before Fe(III) exhaustion. (Fe(III) sensitivity simulations are not shown).

### **3. Validation and sensitivity analysis**

We chose to simulate the microbial activities in test-wells D05 and D08 during the 2007 field experiment in order to validate our model, because they represent the two extreme cases with respect to ammonium availability. The ammonium concentration in D05 is much lower than the ammonium concentration in D08. The competition dynamics are similar to the simulations in the previous section. The *Geobacter* fraction appears to be sensitive to the initial biomass concentration, especially when ammonium is in excess. The simulations initiated with 0.00001 g/L and 0.000001 g/L of biomass agreed well with the experimentally measured microbial fraction in the respective wells (Figure 5), while the simulations initiated with 0.0001 g/L did not. This suggests the cellular density is in the range of  $10^6$  and  $10^7$  cells/L prior to acetate injection, a value that is consistent with previous publications (Yabusaki et al., 2007) and our simulation assumptions in the previous sections. The *Geobacter* fraction is insensitive to the bioavailable Fe(III) concentration. We have also performed sensitivity analysis on the kinetic parameter of *R. ferrireducens* by increasing and decreasing its  $V_{max}$  and  $K_s$  on acetate by 20%. We found no significant changes in the simulation results. (Not shown).

### **4. Changes in the metabolic states**

One advantage of the genome scale dFBA models is their capability to predict changes in metabolic states. We were able to detect the several different growth phases of *G. sulfurreducens* and *R. ferrireducens*. Beyond the donor-limited growth state and acceptor-limited decay state, ammonium-limited states were predicted for both organisms. Although we

do not have ammonium uptake parameters, we can still predict the behavior of the organisms in the extreme cases. For *R. ferrireducens*, a pure maintenance phase is predicted where acetate is oxidized for maintenance purpose only and the biomass flux is zero. *G. sulfurreducens* has an ammonium-limited nitrogen fixation phase. When ammonium becomes limited, *G. sulfurreducens* switches to the nitrogen fixation state at an energetic cost. The energetic cost is reflected in the 30% reduction in growth yield during the nitrogen-fixation phase (Figure 6).

We compared the normal donor-limited growth phase of *G. sulfurreducens* with the nitrogen fixation state (Figure). An increased flux during the nitrogen fixation state is shown in red, whereas a decreased flux is shown in blue. More acetate enters the TCA cycle during the nitrogen fixation state and less acetate enters through acetate kinase, leading to less pyruvate production through pyruvate oxidoreductase. There is also an increase flux through ATP synthase (energy production), as well as through NADH dehydrogenase and cytochrome C reductase (electron transport chain). This indicates that during the nitrogen fixation state, respiration is elevated to provide additional ATP used for nitrogen fixation, at the cost of biomass production.

## DISCUSSION

### 1. Growth Competition

It was previously unknown whether the dominance of *Geobacter* species during bioremediation reflected the pre-existing dominance of *Geobacter* species in uranium-contaminated grounds. The 16S rRNA analysis of sediment samples and nitrogen concentration measurements show that prior to acetate injection, the community distribution seems to be modulated by ammonium concentration — *Geobacter* species have an advantage under low ammonium conditions, while *Rhodoferrax* species have an advantage under high ammonium conditions. As soon as acetate is injected into the ground, *Geobacter* species appear to be dominant regardless of ammonium concentrations, until other factors such as Fe(III) availability limits growth. This shows that the dominance of *Geobacter* species during bioremediation is induced by the acetate injection and does not reflect the community composition prior to injection.

It seems that *Geobacteraceae* and *Rhodoferrix* species have adopted very different evolutionary strategies despite being in the same environment. Thermodynamics dictates that organisms either wastefully utilize resources to maximize specific growth rate, or economically utilize resources to maximize growth yield (Thomas Pfeiffer & Sebastian Bonhoeffer, 2003; T Pfeiffer et al., 2001; Thomas Pfeiffer & Sebastian Bonhoeffer, 2004; Stefan Schuster et al., 2008). From growth kinetics of *G. sulfurreducens* and *R. ferrireducens*, we can see that *G. sulfurreducens* appears to be optimized for faster rate while *R. ferrireducens* is optimized for higher yield, thus we can consider *G. sulfurreducens* as a "rate-strategist" and *R. ferirreducens* as a "yield-strategist". Pfeiffer *et al.* (2001) showed that a high substrate flux condition favors rate-strategists, while yield-strategists thrive under lower substrate flux. (Pfeiffer:2001p581,

Schuster:2007). During uranium bioremediation, the acetate flux to the contaminated ground is very high, thus favoring the rate-optimizing *G. sulfurreducens*. Prior to the acetate injection, the survival of the microorganisms depends on the minute flow of organic chemicals such as glucose and acetate. Since *R. ferrireducens* has high yield on both substrates, it has significant advantage over *Geobacter* species. When ammonium is unlimited, *R. ferrireducens* significantly outcompetes *G. sulfurreducens*. However, since *Rhodoferrax* species cannot fix nitrogen, their growth is limited under low ammonium conditions, allowing *Geobacter* species to succeed. Recent data (unpublished) suggests that it is possible that the subsurface clades of *Geobacteraceae* can use glucose. Therefore, the benefit of *Rhodoferrix*'s capability to use both substrates relative to *Geobacteraceae* is debatable.

## **2. Nitrogen fixation state**

Since nitrogen fixation is associated with an energetic cost, environments with higher ammonium availability will have higher biomass concentrations. During the 2007 field experiment, well D08 had the highest ammonium concentration measurements. Despite having a significantly lower acetate concentration than the other wells due to water flow path, *Geobacteraceae* is significantly more abundant in this well. This suggests that ammonium is a major limiting substrate in anoxic ferric sediments. (Mousser *et al.*, Personal Communication).

The ammonium limitation in the natural environment has a significant impact on the effectiveness of uranium-bioremediation. The rate of uranium reduction can be calculated as the product of specific uranium reduction rate and biomass concentration. During nitrogen fixation, the specific uranium reduction rate can increase due to the up-regulation of respiration, at the expense of biomass production. This hypothesis is supported by experimental data. Well D08

has a significantly lower uranium reduction rate compared to the wells with lower ammonium concentrations, despite having the highest biomass concentration, possibly due to the increased respiration in the wells with limited ammonium. However, although D05 has a lower ammonium concentration than D02, D02 has a higher uranium reduction rate. The predicted respiratory up-regulation during the nitrogen fixation of *G. sulfurreducens* as well as the prediction of a maintenance state for *R. ferrireducens* illustrate a significant advantage of using dFBA models — their ability to detect metabolic changes in response to environmental cues. Ultimately, such models can be integrated with dynamic optimization techniques to predict the optimal ammonium concentrations at which the total uranium reduction over time is maximized. This insight also suggests bioremediation strategies that artificially reduce the ammonium concentration to induce nitrogen fixation at an energetic cost, thus achieving a higher uranium reduction rate. This strategy is reminiscent of a recent study where the introduction of a futile cycle in *G. sulfurreducens* increased the energy demand and resulted in increased respiration, but lowered biomass yields (Izallalen et al., 2008).

### **3. Understanding bioremediation**

Since the community composition shifts in favor of *G. sulfurreducens* immediately after acetate injection begins, *R. ferrireducens* plays a minor role in the overall consumption of acetate, ammonium and ferric iron. We can assume that uranium bioremediation is dominated by the interactions between *Geobacteraceae* and the environment, so we focus our attention on the behavior of *Geobacter* species during acetate injection. Our simulations suggest that the rapid utilization and exhaustion of bioavailable ferric iron lead to the decay of *Geobacter* species; this agrees with the previous hypothesis that the decrease in uranium removal upon



prolonged acetate injection is caused by iron limitation. Continued acetate injection after the exhaustion of ferric iron leads to an excess of acetate, which stimulates the growth of other acetate oxidizing organisms. While exhaustion of the electron acceptor limits the growth of *Geobacter* species, other organisms can outcompete them for acetate, thereby hindering uranium bioremediation.

Sensitivity analyses suggest that both the acetate injection rate and the bio-available ferric iron concentration modulate the length of time *Geobacter* species can maintain their dominance. We cannot manipulate Fe(III) availability in nature easily; however, we can adjust the rate of acetate injection. The 2007 field experiment shows termination of acetate at day 10 does not lead to an immediate termination of uranium reduction, since acetate remains in the system until washed out by ground water flow. One strategy might be to decrease the acetate injection rate prior to Fe(III) depletion. Since *Geobacter* species will still dominate the community, the lowered acetate flux will be used for uranium reduction. There will not be enough acetate to stimulate the growth of other organisms. Although such a strategy is conceptually viable, the predictive design of such a strategy requires the aid of a computational model that integrates microbial physiology with geochemistry as well as the expansion of the current modeling effort to incorporate the growth physiology of sulfate reducers such as *Desulfobacter* species (cite a reference).

## REFERENCES

- Anderson, R. T., Vrionis, H. A., Ortiz-Bernad, I., Resch, C. T., Long, P. E., Dayvault, R., Karp, K., Marutzky, S., Metzler, D. R., Peacock, A., White, D. C., Lowe, M., & Lovley, D. R. 2003. Stimulating the in situ activity of *Geobacter* species to remove uranium from the groundwater of a uranium-contaminated aquifer. *Applied and Environmental Microbiology* **69**: 5884-91.
- Anesiadis, N., Cluett, W. R., & Mahadevan, R. 2008. Dynamic metabolic engineering for increasing bioprocess productivity. *Metabolic Engineering*. Retrieved August 16, 2008, from <http://www.ncbi.nlm.nih.gov/pubmed/18606241>
- Burgard, A. P., Pharkya, P., & Maranas, C. D. 2003. Optknock: a bilevel programming framework for identifying gene knockout strategies for microbial strain optimization. *Biotechnology and Bioengineering* **84**: 647-57.
- Chang, Y., Long, P. E., Geyer, R., Peacock, A. D., Resch, C. T., Sublette, K., Pfiffner, S., Smithgall, A., Anderson, R. T., Vrionis, H. A., Stephen, J. R., Dayvault, R., Ortiz-Bernad, I., Lovley, D. R., & White, D. C. 2005. Microbial incorporation of <sup>13</sup>C-labeled acetate at the field scale: detection of microbes responsible for reduction of U(VI). *Environmental Science & Technology* **39**: 9039-48.
- Chaudhuri, S. K., & Lovley, D. R. 2003. Electricity generation by direct oxidation of glucose in mediatorless microbial fuel cells. *Nature Biotechnology* **21**: 1229-32.
- Cummings, D. E., Snoeyenbos-West, O. L., Newby, D. T., Niggemyer, A. M., Lovley, D. R., Achenbach, L. A., & Rosenzweig, R. F. 2003. Diversity of *Geobacteraceae* species inhabiting metal-polluted freshwater lake sediments ascertained by 16S rDNA analyses. *Microbial Ecology* **46**: 257-69.
- Edwards, J. S., Ibarra, R. U., & Palsson, B. O. 2001. In silico predictions of *Escherichia coli* metabolic capabilities are consistent with experimental data. *Nature Biotechnology* **19**: 125-30.
- Edwards, J. S., Covert, M., & Palsson, B. 2002. Metabolic modelling of microbes: the flux-balance approach. *Environmental Microbiology* **4**: 133-40.
- Esteve-Núñez, A., Rothermich, M., Sharma, M., & Lovley, D. 2005. Growth of *Geobacter sulfurreducens* under nutrient-limiting conditions in continuous culture. *Environmental Microbiology* **7**: 641-8.
- Feist, A. M., Henry, C. S., Reed, J. L., Krummenacker, M., Joyce, A. R., Karp, P. D., Broadbelt, L. J., Hatzimanikatis, V., & Palsson, B. Ø. 2007. A genome-scale metabolic reconstruction for *Escherichia coli* K-12 MG1655 that accounts for 1260 ORFs and thermodynamic information. *Molecular Systems Biology* **3**: 121.

- Feist, A. M., & Palsson, B. Ø. 2008. The growing scope of applications of genome-scale metabolic reconstructions using *Escherichia coli*. *Nature Biotechnology* **26**: 659-67.
- Finneran, K. T., Johnsen, C. V., & Lovley, D. R. 2003. *Rhodoferrax ferrireducens* sp. nov., a psychrotolerant, facultatively anaerobic bacterium that oxidizes acetate with the reduction of Fe(III). *International Journal of Systematic and Evolutionary Microbiology* **53**: 669-73.
- de Graaf, W., Wellsbury, P., Parkes, R. J., & Cappenberg, T. E. 1996. Comparison of Acetate Turnover in Methanogenic and Sulfate-Reducing Sediments by Radiolabeling and Stable Isotope Labeling and by Use of Specific Inhibitors: Evidence for Isotopic Exchange. *Applied and Environmental Microbiology* **62**: 772-777.
- Hjersted, J. L., Henson, M. A., & Mahadevan, R. 2007. Genome-scale analysis of *Saccharomyces cerevisiae* metabolism and ethanol production in fed-batch culture. *Biotechnology and Bioengineering* **97**: 1190-204.
- Ibarra, R. U., Edwards, J. S., & Palsson, B. O. 2002. *Escherichia coli* K-12 undergoes adaptive evolution to achieve in silico predicted optimal growth. *Nature* **420**: 186-9.
- Izallalen, M., Mahadevan, R., Burgard, A., Postier, B., Didonato, R., Sun, J., Schilling, C. H., & Lovley, D. R. 2008. *Geobacter sulfurreducens* strain engineered for increased rates of respiration. *Metabolic Engineering*. Retrieved August 16, 2008, from <http://www.ncbi.nlm.nih.gov/pubmed/18644460>
- King, G. M., & Klug, M. J. 1982. Glucose Metabolism in Sediments of a Eutrophic Lake: Tracer Analysis of Uptake and Product Formation. *Applied and Environmental Microbiology* **44**: 1308-1317.
- Konopka, A. 2006. Microbial ecology: Searching for principles. *Microbe* **1**: 175-179.
- Lee, J. M., Gianchandani, E. P., & Papin, J. A. 2006. Flux balance analysis in the era of metabolomics. *Brief Bioinform*: bbl007.
- Lovley, D. R. 2003. Cleaning up with genomics: applying molecular biology to bioremediation. *Nature Reviews. Microbiology* **1**: 35-44.
- Lovley, D. R., Holmes, D. E., & Nevin, K. P. 2004. Dissimilatory Fe(III) and Mn(IV) reduction. *Advances in Microbial Physiology* **49**: 219-86.
- Lovley, D. R., & Phillips, E. J. P. 1989. Requirement for a Microbial Consortium To Completely Oxidize Glucose in Fe(III)-Reducing Sediments. *Applied and Environmental Microbiology* **55**: 3234-3236.

- Luo, R., Liao, S., Tao, G., Li, Y., Zeng, S., Li, Y., & Luo, Q. 2006. Dynamic analysis of optimality in myocardial energy metabolism under normal and ischemic conditions. *Molecular Systems Biology* **2**: 2006.0031.
- Mahadevan, R., Bond, D. R., Butler, J. E., Esteve-Núñez, A., Coppi, M. V., Palsson, B. O., Schilling, C. H., & Lovley, D. R. 2006. Characterization of metabolism in the Fe(III)-reducing organism *Geobacter sulfurreducens* by constraint-based modeling. *Applied and Environmental Microbiology* **72**: 1558-68.
- Mahadevan, R., Edwards, J. S., & Doyle, F. J. 2002. Dynamic flux balance analysis of diauxic growth in *Escherichia coli*. *Biophysical Journal* **83**: 1331-40.
- McMahon, K. D., Martin, H. G., & Hugenholtz, P. 2007. Integrating ecology into biotechnology. *Current Opinion in Biotechnology* **18**: 287-92.
- Méthé, B. A., Nelson, K. E., Eisen, J. A., Paulsen, I. T., Nelson, W., Heidelberg, J. F., Wu, D., Wu, M., Ward, N., Beanan, M. J., Dodson, R. J., Madupu, R., Brinkac, L. M., Daugherty, S. C., DeBoy, R. T., et al. 2003. Genome of *Geobacter sulfurreducens*: metal reduction in subsurface environments. *Science (New York, N.Y.)* **302**: 1967-9.
- N'Guessan, A. L., Vrionis, H. A., Resch, C. T., Long, P. E., & Lovley, D. R. 2008. Sustained removal of uranium from contaminated groundwater following stimulation of dissimilatory metal reduction. *Environmental Science & Technology* **42**: 2999-3004.
- Pfeiffer, T., Schuster, S., & Bonhoeffer, S. 2001. Cooperation and competition in the evolution of ATP-producing pathways. *Science (New York, N.Y.)* **292**: 504-7.
- Pfeiffer, T., & Bonhoeffer, S. 2003. An evolutionary scenario for the transition to undifferentiated multicellularity. *Proceedings of the National Academy of Sciences of the United States of America* **100**: 1095-8.
- Pfeiffer, T., & Bonhoeffer, S. 2004. Evolution of cross-feeding in microbial populations. *The American Naturalist* **163**: E126-35.
- Pharkya, P., Burgard, A. P., & Maranas, C. D. 2003. Exploring the overproduction of amino acids using the bilevel optimization framework OptKnock. *Biotechnology and Bioengineering* **84**: 887-99.
- Pharkya, P., & Maranas, C. D. 2006. An optimization framework for identifying reaction activation/inhibition or elimination candidates for overproduction in microbial systems. *Metabolic Engineering* **8**: 1-13.
- Price, N. D., Reed, J. L., & Palsson, B. Ø. 2004. Genome-scale models of microbial cells: evaluating the consequences of constraints. *Nature Reviews. Microbiology* **2**: 886-97.

- Reed, J. L., & Palsson, B. Ø. 2003. Thirteen years of building constraint-based in silico models of *Escherichia coli*. *Journal of Bacteriology* **185**: 2692-9.
- Reed, J. L., Vo, T. D., Schilling, C. H., & Palsson, B. O. 2003. An expanded genome-scale model of *Escherichia coli* K-12 (iJR904 GSM/GPR). *Genome Biology* **4**: R54.
- Rittmann, B. E., & McCarty, P. L. 2001. *Environmental Biotechnology*.
- Schuster, S., Pfeiffer, T., & Fell, D. A. 2008. Is maximization of molar yield in metabolic networks favoured by evolution? *Journal of Theoretical Biology* **252**: 497-504.
- Segura, D., Mahadevan, R., Juárez, K., & Lovley, D. R. 2008. Computational and experimental analysis of redundancy in the central metabolism of *Geobacter sulfurreducens*. *PLoS Computational Biology* **4**: e36.
- Stolyar, S., Van Dien, S., Hillesland, K. L., Pinel, N., Lie, T. J., Leigh, J. A., & Stahl, D. A. 2007. Metabolic modeling of a mutualistic microbial community. *Molecular Systems Biology* **3**: 92.
- Tajima, K., Arai, S., Ogata, K., Nagamine, T., Matsui, H., Nakamura, M., Aminov, R. I., & Benno, Y. 2000. Rumen Bacterial Community Transition During Adaptation to High-grain Diet. *Anaerobe* **6**: 273-284.
- VanBriesen, J. M. 2002. Evaluation of methods to predict bacterial yield using thermodynamics. *Biodegradation* **13**: 171-90.
- Vrionis, H. A., Anderson, R. T., Ortiz-Bernad, I., O'Neill, K. R., Resch, C. T., Peacock, A. D., Dayvault, R., White, D. C., Long, P. E., & Lovley, D. R. 2005. Microbiological and geochemical heterogeneity in an in situ uranium bioremediation field site. *Applied and Environmental Microbiology* **71**: 6308-18.
- Warren, P. B., & Jones, J. L. 2007. Duality, thermodynamics, and the linear programming problem in constraint-based models of metabolism. *Physical Review Letters* **99**: 108101.
- Yabusaki, S. B., Fang, Y., Long, P. E., Resch, C. T., Peacock, A. D., Komlos, J., Jaffe, P. R., Morrison, S. J., Dayvault, R. D., White, D. C., & Anderson, R. T. 2007. Uranium removal from groundwater via in situ biostimulation: Field-scale modeling of transport and biological processes. *Journal of Contaminant Hydrology* **93**: 216-35.

## **ACKNOWLEDGEMENT**

This research was supported by the Office of Science (BER), U.S. Department of Energy, Cooperative Agreement No. DE-FC02-02ER63446 and Grant No. DE-FG02-07ER64367, as well Canada Foundation for Innovation and University of Toronto Open Fellowship. Special thanks: Laurence Yang for insightful discussions and Emma Janssen for grammatical corrections.

Figure 1. Conceptual model of uranium-bioremediation.

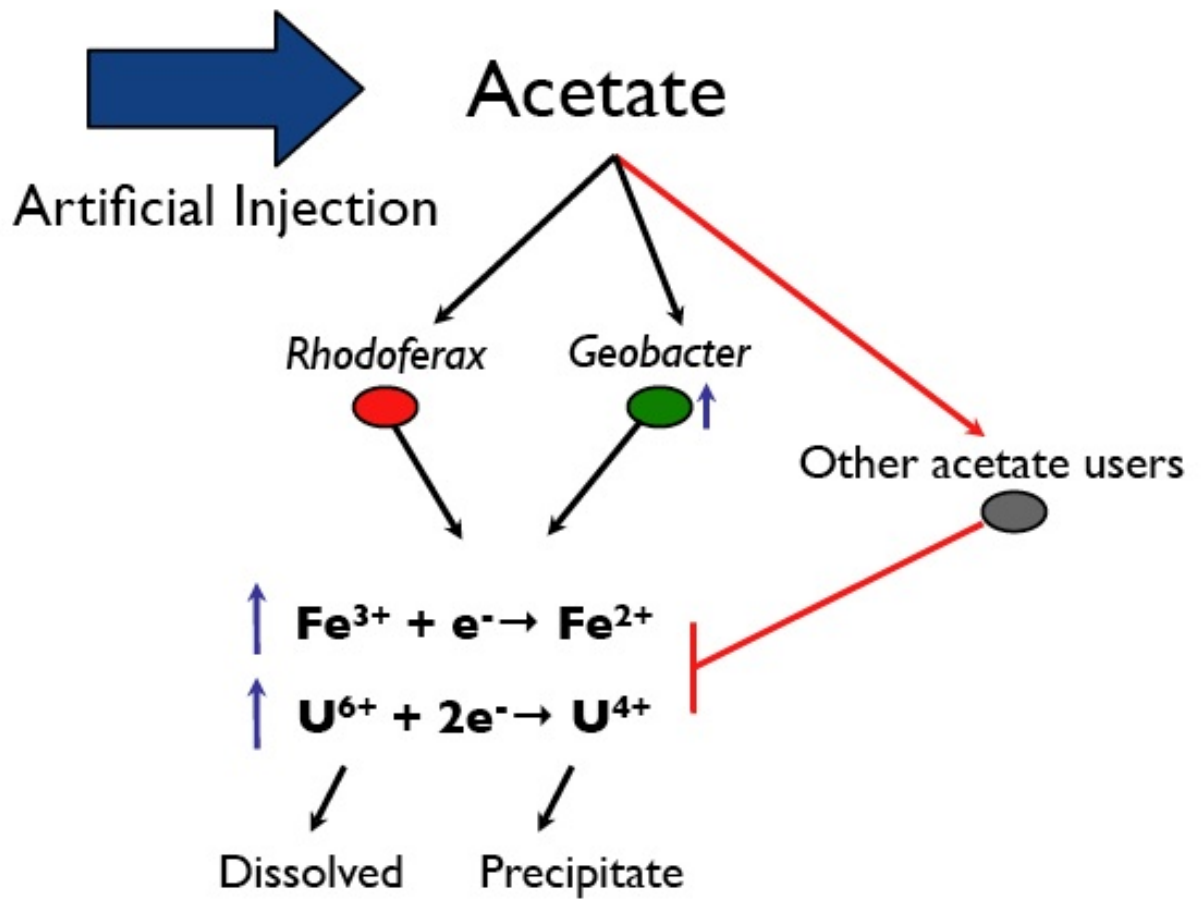


Figure 2. The DMMM framework applied to the modeling of iron reducers.

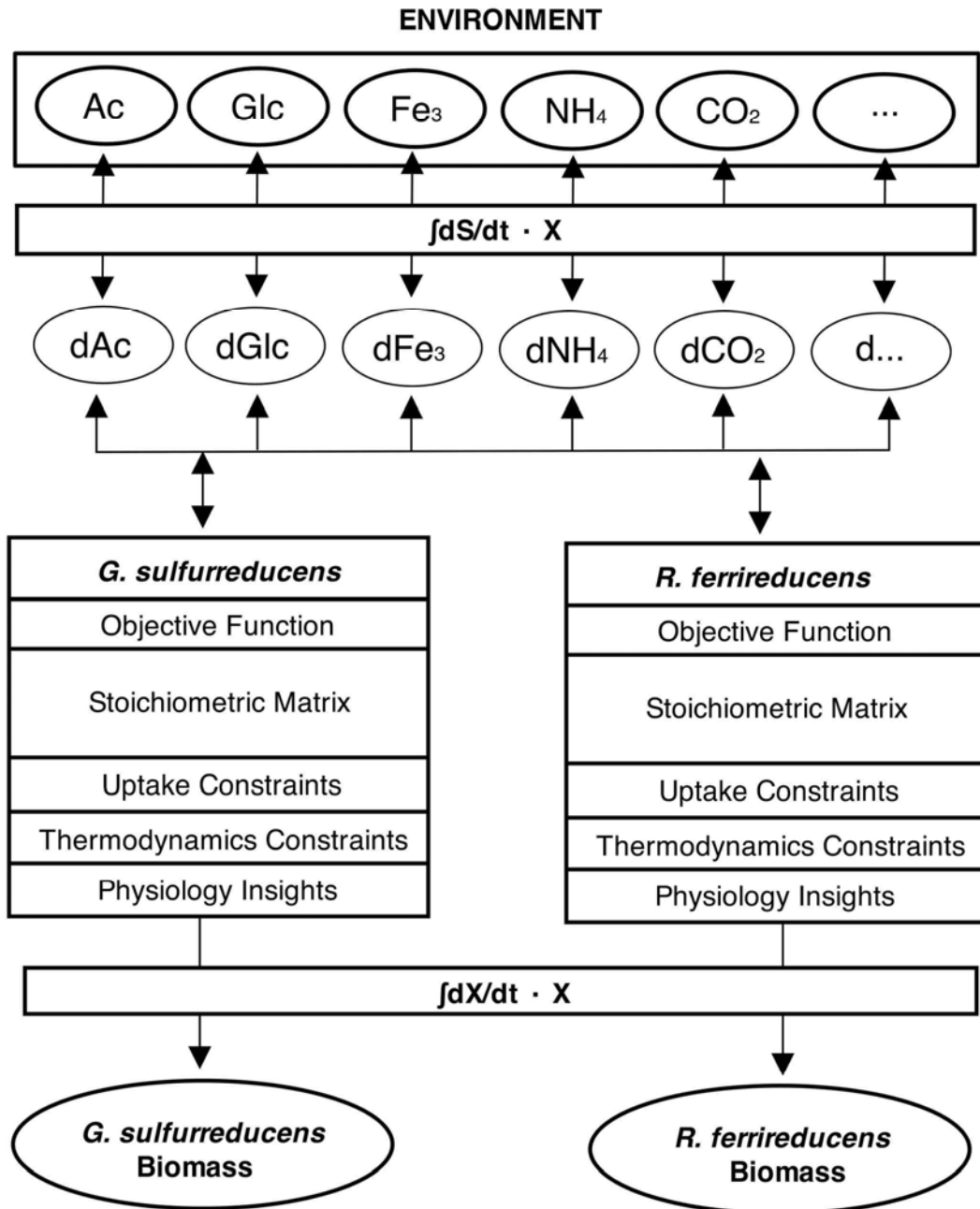




Figure 3. Iron-reducer competition prior to acetate amendment.

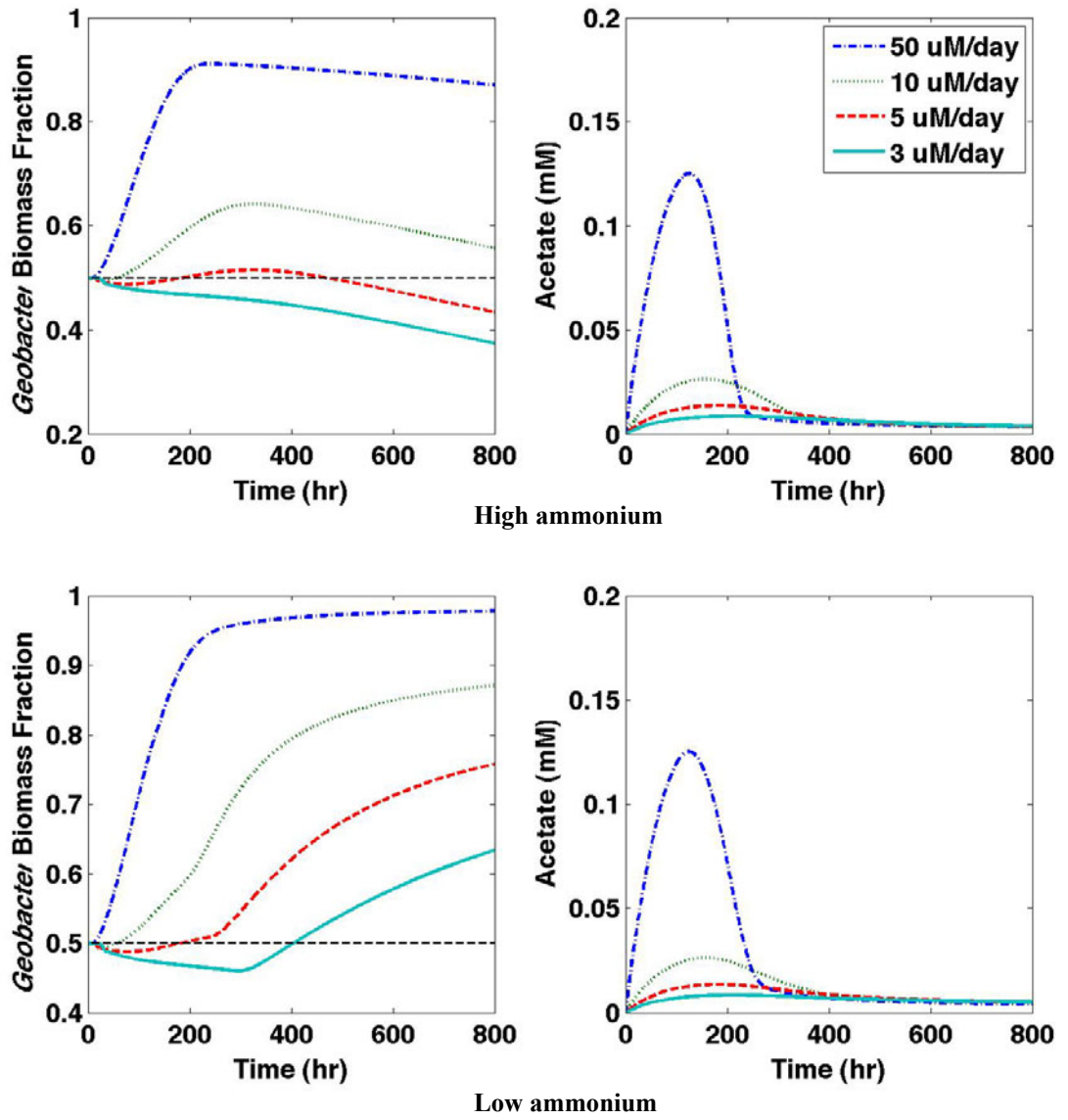


Figure 4. Iron-reducer competition prior during acetate amendment.

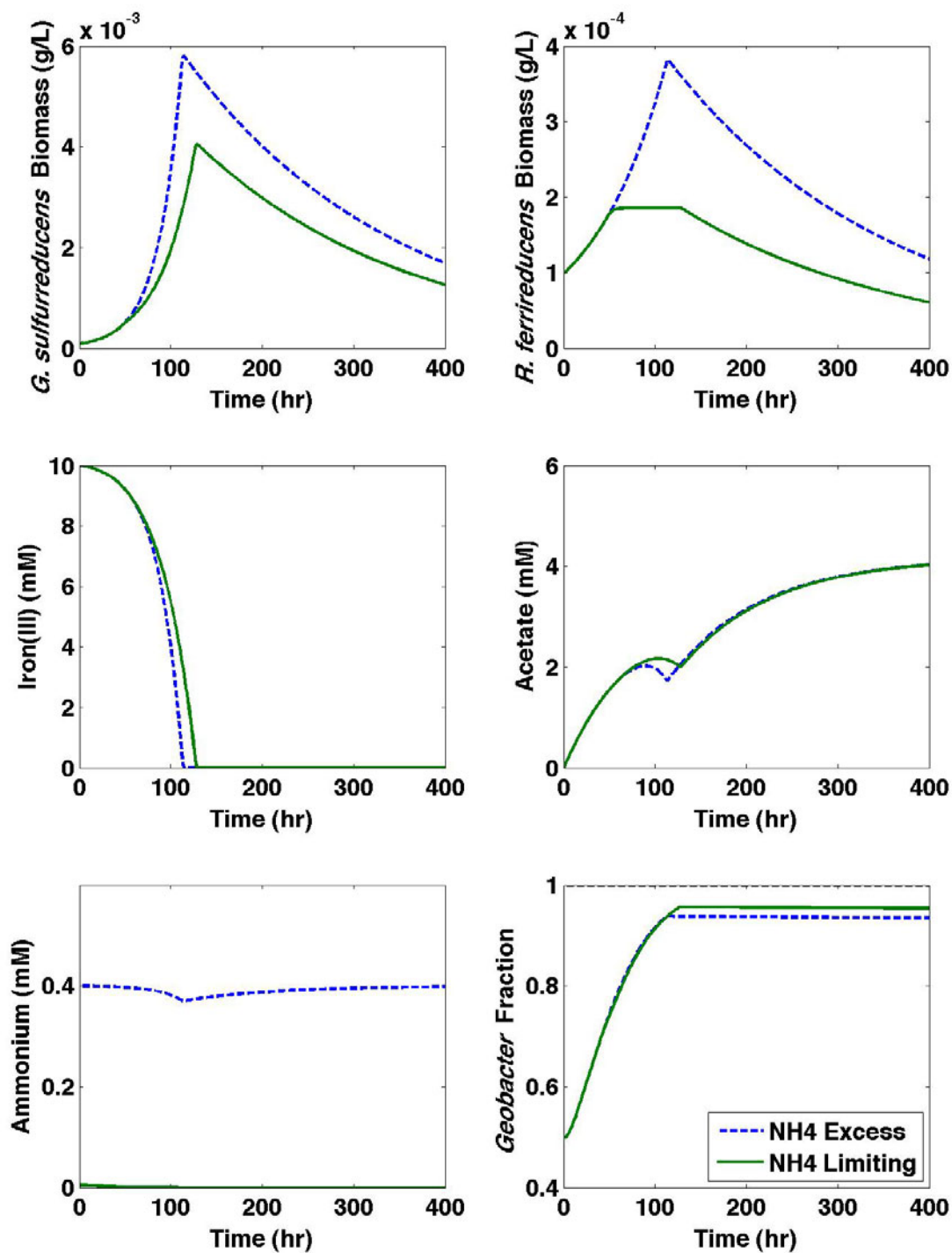


Figure 5. Model validation. ▲ is the experimentally measured *Geobacter* fraction.

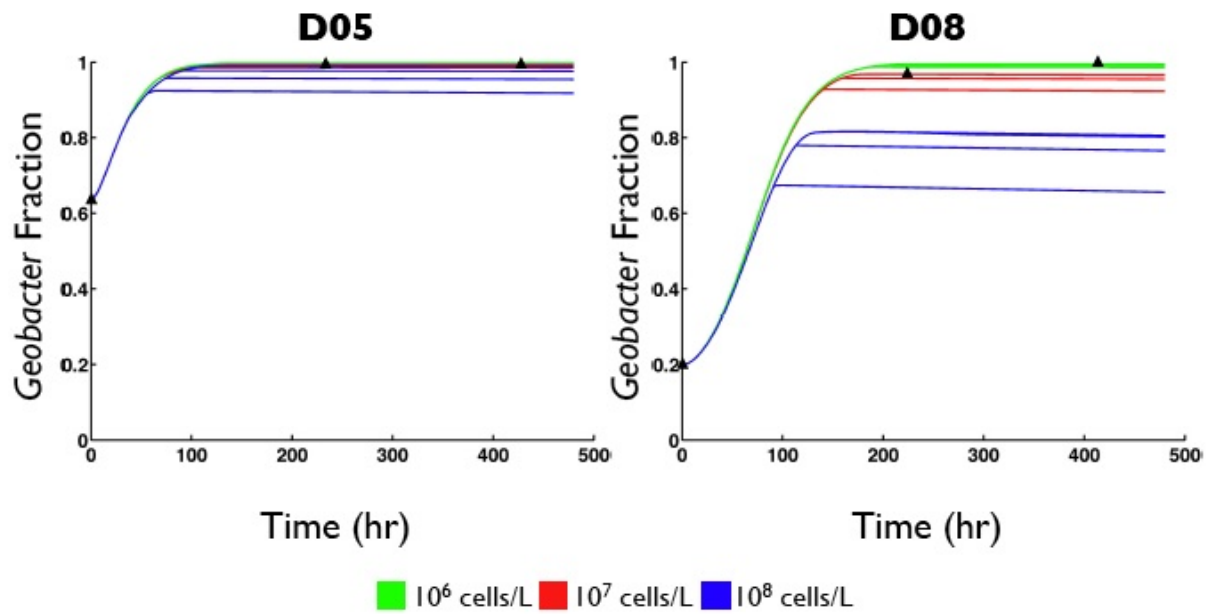


Figure 6. Normal growth vs. nitrogen-fixation dependent growth of *G. sulfurreducens*

